Fitting a self-interacting dark matter model to data ranging from satellite galaxies to galaxy clusters

Sudhakantha Girmohanta[1,2] and Robert Shrock[1]

[1]*C. N. Yang Institute for Theoretical Physics and Department of Physics and Astronomy, Stony Brook University, Stony Brook, New York 11794, USA*

[2]*Tsung-Dao Lee Institute and School of Physics and Astronomy, Shanghai Jiao Tong University, 800 Dongchuan Road, Shanghai 200240, China*

(Received 3 October 2022; accepted 13 February 2023; published 8 March 2023)

We present a fit to observational data in an asymmetric self-interacting dark matter model using our recently calculated cross sections that incorporate both t-channel and u-channel exchanges in the scattering of identical particles. We find good fits to the data ranging from dwarf galaxies to galaxy clusters and equivalent relative velocities from ~ 20 km/s to $\gtrsim 10^3$ km/s. We compare our results with previous fits that used only t-channel exchange contributions to the scattering.

DOI: 10.1103/PhysRevD.107.063006

I. INTRODUCTION

There is strong evidence for dark matter (DM), comprising about 85% of the matter in the Universe. Cold dark matter (CDM) can account for structures on length scales larger than ~ 10 Mpc [1–6] (reviews include [7–13]). However, problems have been noted with fits to observational data on shorter length scales of ~ 1–100 kpc using early CDM simulations without baryon feedback [14–16]. These problems included the prediction of greater density in the central region of galaxies than was observed (the core-cusp problem), a greater number of dwarf satellite galaxies than were seen (the missing satellite problem), and the so-called "too big to fail" problem pertaining to star formation in dwarf satellite galaxies. Models with self-interacting dark matter (SIDM) have been shown to avoid these problems (some reviews include [17–19]). The extension of cold dark matter N-body simulations to include baryon feedback can ameliorate these problems with pure CDM simulations [20–33]. Nevertheless, cosmological models with SIDM are of considerable interest in their own right and have been the subject of intensive study [17–19,34–89].

In the framework of a particle theory of dark matter, the rate of DM-DM scatterings is given by $\Gamma = (\sigma/m_{\rm DM})v_{\rm rel}\rho_{\rm DM}$, where σ, $m_{\rm DM}$, $v_{\rm rel}$, and $\rho_{\rm DM}$ are the DM-DM scattering cross section, DM particle mass, relative velocity of two colliding DM particles, and DM mass density, respectively. Fits to observational data on the scale of ~ 1–10 kpc, with velocities $v_{\rm rel} \sim 20$–200 km/s, yield values $\sigma/m_{\rm DM} \sim 1$ cm^2/g, while fits to observations of galaxy clusters on distance scales of several Mpc and $v_{\rm rel} \sim O(10^3)$ km/s yield smaller values of $\sigma/m_{\rm DM} \sim 0.1$ cm^2/g. This implies that viable SIDM models should have cross sections that decrease as a function of $v_{\rm rel}$. This property can be achieved in models in which DM particles, denoted χ here, interact via exchange of a light (Lorentz scalar or vector) mediator field, generically denoted ξ.

In models with asymmetric dark matter (ADM), after the number asymmetry is established in the early Universe, the DM self-interaction occurs via the reaction

$$\chi + \chi \to \chi + \chi. \tag{1.1}$$

Because of the identical particles in the final state, a proper treatment necessarily includes both the t-channel and the u-channel contributions to the scattering amplitude. In [89], we presented differential and integrated cross sections for the reaction (1.1) with both the t-channel and u-channel terms included and discussed the differences with respect to previous calculations that included only the t-channel term. Identical-particle effects have also been noted in [58,88] in a field-theoretic context and in [48,79] in the context of solutions of the Schrödinger equation for potential scattering. An interesting question raised by our work in [89] is the following: how do the fits to observational data change when one uses the cross section with both t-channel and u-channel contributions to the scattering, as contrasted with previous fits that used only the t-channel contributions? In the present paper we address this question using the same observational dataset that was analyzed in [52].

II. CROSS SECTIONS

First, we review the basic properties of the SIDM model with asymmetric dark matter that we used in [89]. In this model, the dark matter particle χ is a spin-1/2 Dirac fermion, and the mediator, ξ, is a real scalar, $\xi = \phi$, or a vector, $\xi = V$. Both χ and ξ are singlets under the Standard Model (SM). For the version of the model with a real scalar mediator, we take the χ-ϕ interaction to be of Yukawa form, as described by the interaction Lagrangian $\mathcal{L}_{\rm Yuk} = y_\chi[\bar{\chi}\chi]\phi$. In the version with a vector mediator, the DM fermion χ is assumed to be charged under a $\mathrm{U}(1)_V$ gauge symmetry with gauge field V and gauge coupling g. Since only the product of the $\mathrm{U}(1)_V$ charge of χ times g occurs in the covariant derivative in this theory, we may, without loss of generality, take this charge to be unity and denote the product as g_χ. The corresponding interaction Lagrangian is $\mathcal{L}_{\bar{\chi}\chi V} = g_\chi[\bar{\chi}\gamma_\mu\chi]V^\mu$. A Higgs-type mechanism is assumed to break the $\mathrm{U}(1)_V$ symmetry and give a mass m_V to the gauge field V. For compact notation, we use the same symbol, α_χ, to denote $y_\chi^2/(4\pi)$ for the case of a scalar mediator and $g_\chi^2/(4\pi)$ for the case of a vector mediator. We assume that the kinetic mixing of V with the SM hypercharge gauge boson is negligibly small. (For an example of how this mixing can be suppressed in a DM model with specified ultraviolet physics, see, e.g., [90].) In [89] the illustrative set of values $m_\chi = 5\,\mathrm{GeV}$, $m_\xi = 5\,\mathrm{MeV}$, and $\alpha_\chi = 3\times 10^{-4}$ was used. Below we will show that this choice is consistent with the fit to astronomical data that we perform here.

We restrict to the case where α_χ is small enough so that lowest-order perturbation theory provides a reliable description of the physics. As was shown in [89], the parameter choice used there satisfies this restriction while simultaneously yielding sufficient depletion of the $\bar{\chi}$ number density in the early Universe to produce the assumed number asymmetry in our ADM model. For further details on our model, we refer the reader to [89].

The amplitude for the reaction (1.1) is $\mathcal{M} = \mathcal{M}^{(t)} - \mathcal{M}^{(u)}$, where $\mathcal{M}^{(t)}$ and $\mathcal{M}^{(u)}$ are the t-channel and u-channel contributions, respectively, and the minus sign embodies the effect of interchange of identical fermions in the final state. Let us define a prefactor σ_0 and dimensionless ratio r as

$$\sigma_0 = \frac{\alpha_\chi^2 m_\chi^2}{m_\xi^4}, \qquad r = \left(\frac{\beta_{\rm rel} m_\chi}{m_\xi}\right)^2, \tag{2.1}$$

where $\beta_{\rm rel} = v_{\rm rel}/c$. For all the relevant data, the values of $v_{\rm rel}$ are nonrelativistic (NR). In [89] we calculated the differential cross section in the center-of-mass (c.m.), $d\sigma_{\rm c.m.}/d\Omega$, for the reaction (1.1) with both scalar and vector mediators in the regime where the Born approximation is valid. In the NR limit relevant to fitting data, the results for the scalar and vector mediators are equal and are [89]

$$\left(\frac{d\sigma}{d\Omega}\right)_{\rm c.m.,NR} = \sigma_0\left[\frac{1}{(1+r\sin^2(\theta/2))^2} + \frac{1}{(1+r\cos^2(\theta/2))^2} - \frac{1}{(1+r\sin^2(\theta/2))(1+r\cos^2(\theta/2))}\right]. \tag{2.2}$$

The terms on the right-hand side of Eq. (2.2) are from $|\mathcal{M}^{(t)}|^2$, $|\mathcal{M}^{(u)}|^2$, and $[\mathcal{M}^{(t)*}\mathcal{M}^{(u)} + \mathcal{M}^{(u)*}\mathcal{M}^{(t)}]$, respectively. The angular integrals of these terms are correspondingly denoted as $\sigma^{(t)}$, $\sigma^{(u)}$, and $\sigma^{(tu)}$. Because of the identical particles in the final state, a scattering event in which a scattered χ particle emerges at angle θ is indistinguishable from one in which a scattered χ emerges at angle $\pi - \theta$. The total cross section for the reaction (1.1) thus involves a symmetry factor of $1/2$ to compensate for the double-counting involved in the integration over the range $\theta \in [0, \pi]$:

$$\sigma = \frac{1}{2}\int d\Omega \left(\frac{d\sigma}{d\Omega}\right)_{\rm c.m.}. \tag{2.3}$$

Owing to the symmetry $(\frac{d\sigma}{d\Omega})_{\rm c.m.}(\theta) = (\frac{d\sigma}{d\Omega})_{\rm c.m.}(\pi - \theta)$, this is equivalent to a polar angle integration from 0 to $\pi/2$.

To describe the thermalization effects of DM-DM scattering, cross sections that give greater weight to large-angle scattering have also been used in fits to data. These include the transfer (T) cross section $d\sigma_T/d\Omega = (1-\cos\theta)(d\sigma/d\Omega)_{\rm c.m.}$ and the viscosity (V) cross section $d\sigma_V/d\Omega = (1-\cos^2\theta)(d\sigma/d\Omega)_{\rm c.m.}$. These have the respective weighting factors $w_T(\theta) = 1-\cos\theta$ and $w_V(\theta) = 1-\cos^2\theta$, as indicated. Reference [46] suggested the use of the viscosity cross section σ_V for studies of SIDM thermalization effects, and recently, Ref. [88] finds that σ_V provides a very good description of thermalization effect of SIDM scattering. However, since σ_T has been used in a number of past fits to observational data, we include results for it here for completeness. We obtained the integrated cross sections [given as Eqs. (4.30) and (4.38) in [89]]

$$\sigma = \sigma_T = 4\pi\sigma_0\left[\frac{1}{1+r} - \frac{\ln(1+r)}{r(2+r)}\right] \tag{2.4}$$

and

$$\sigma_V = \frac{8\pi\sigma_0}{r^2}\left[-5 + \frac{2(5+5r+r^2)\ln(1+r)}{(2+r)r}\right]. \tag{2.5}$$

For a given weighting factor, the integrals of the terms $(d\sigma/d\Omega)_{\rm c.m.}$ were denoted $\sigma^{(t)}$, $\sigma^{(u)}$, and $\sigma^{(tu)}$ and analytic expressions for these were given for $\sigma = \sigma_T$ and σ_V in our previous work [89]. We note that (when one includes both t-channel and u-channel contributions) since the weighting factor $w_T(\theta) = (1-\cos\theta)$ has no net effect in suppressing

contributions from scattering events that do not produce thermalization, it follows that σ_T could overestimate the thermalization effect from SIDM self-scattering.

In the literature, in the same NR Born regime for the reaction (1.1) a formula was used for the differential cross section of reaction (1.1) that implicitly assumed that the colliding particles were distinguishable [e.g., Eq. (5) in [18]], namely (in our notation)

$$\left(\frac{d\sigma}{d\Omega}\right)_{\text{c.m.},t} = \frac{\sigma_0}{(1 + r\sin^2(\theta/2))^2}. \tag{2.6}$$

The integrals $\sigma = \int d\Omega\, w(\theta)(d\sigma/d\Omega)_{\text{c.m.}}$ with the respective weighting factors [again assuming distinguishable particles in reaction (1.1)] yielded results for σ, σ_T, and σ_V, in particular, the following result for σ_T [Eq. (5) in [39], denoted FKY, which is the same as Eq. (A1) in [45], denoted TYZ and Eq. (6) in [46]]

$$\sigma_{T,\text{FKY,TYZ}} = \frac{8\pi\sigma_0}{r}\left[-\frac{1}{1+r} + \frac{\ln(1+r)}{r}\right]. \tag{2.7}$$

In [89] we showed that

$$\sigma_{T,\text{FKY,TYZ}} = 2\sigma^{(t)}, \tag{2.8}$$

where $\sigma^{(t)}$ was given as Eq. (4.27) in [89], and the factor of 2 difference is due to the fact that the correct calculation divides by $1/2$ to take account of the identical particles in the final state. For brevity, we denote $\sigma_{T,\text{FKY,TYZ}} \equiv \sigma_{T,\text{lit}}$(lit = cited literature).

Following the same procedure as for $\sigma_{T,\text{lit}}$, from Eq. (2.6), one would get

$$\sigma_{V,\text{lit}} = \frac{16\pi\sigma_0}{r^2}\left[-2 + (2+r)\frac{\ln(1+r)}{r}\right]. \tag{2.9}$$

This is twice as large as the term $\sigma_V^{(t)}$ that entered into the full viscosity cross section $\sigma_V = \sigma_V^{(t)} + \sigma_V^{(u)} + \sigma_V^{(tu)}$ that we calculated in [89] [see Eqs. (4.36) and (4.38) in [89]]. The origin of the factor 2 difference is again that when one takes account of the identical particles in the final state, the angular integral (2.3) involves a factor of $1/2$. In addition to [89], more recent studies [58,79,88] have taken account of the indistinguishability of the χ particles in the reaction (1.1). However, we are not aware of published fits to observational datasets used in [52,62] using the SIDM velocity-dependent cross sections in the Born regime that compare fitted values obtained from calculations using cross sections with t-channel and u-channel terms included, as compared to cross sections that only included the t-channel terms. We thus proceed with these comparative fits.

III. FITS TO OBSERVATIONAL DATA

We now address the question of how the fit to data changes when one uses the cross sections from [89] with both t-channel and u-channel contributions to the reaction (1.1). In our main comparison, for definiteness, we use the same set of data from dwarfs, low surface brightness (LSB) galaxies, and galaxy clusters as in [52]. This dataset includes (i) five dwarfs from THINGS (The H I Nearby Galaxy Survey) [91], namely IC 2574, NGC 2366, Holmberg II, M81 dwB, and DDO 154, indicated in red in Figs. 1(a) and 1(b); (ii) seven LSB galaxies from [92], namely UGC 4325, F563-V2, F563-1, F568-3, UGC 5750, F583-4, and F583-1, indicated in blue in Figs. 1(a) and 1(b); and (iii) six relaxed galaxy clusters from [93,94], namely

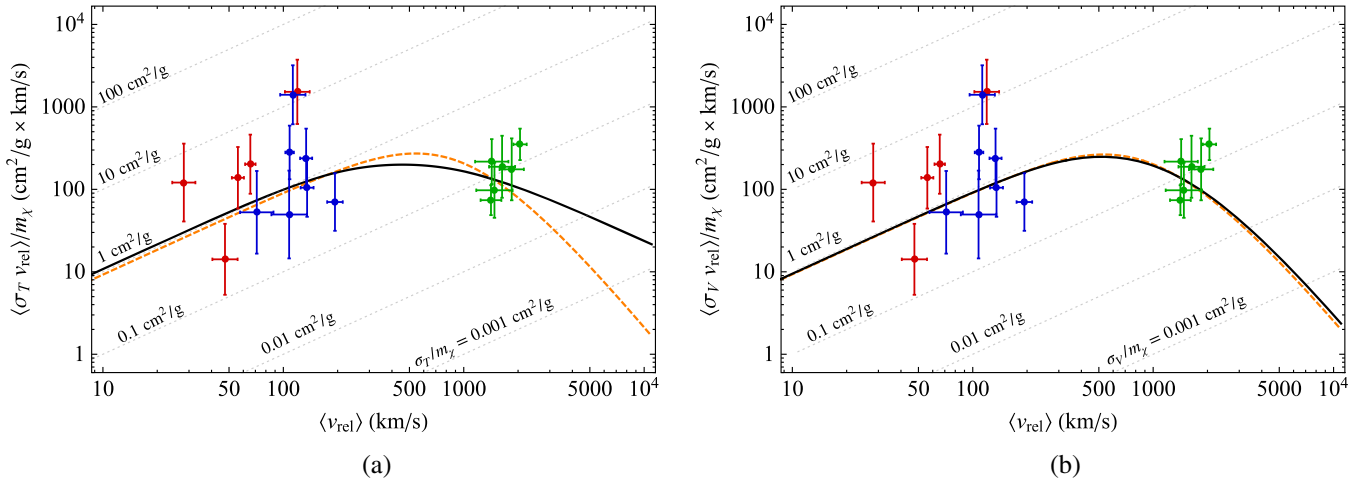

FIG. 1. Fits (black curves) of our (a) σ_T/m_χ and (b) σ_V/m_χ to observational data, where σ_T and σ_V are given in Eqs. (2.4) and (2.5). The data are from dwarfs (red), LSB galaxies (blue), and galaxy clusters (green) as in Ref. [52]. For comparison, fits to this dataset with σ_T and σ_V from Eqs. (2.7) and (2.9), based on Eq. (2.6), are shown as the dashed orange curves. Note that Ref. [88] finds that σ_V provides a better description of thermalization effects due to SIDM scattering than σ_T.

MS2137, A611, A963, A2537, A2667, and A2390, indicated in green in Figs. 1(a) and 1(b). Of these, the galaxy clusters are at distances from us of several hundred Mpc, the LSB galaxies are at distances $\sim O(10)$ Mpc, and the dwarfs are at distances of approximately 3–5 Mpc. This choice of dwarf galaxies considered in [52] has the merit that these are "field" dwarfs located sufficiently far from the Milky Way that they are less subject to the complication of environmental effects, such as possible tidal stripping, than dwarfs closer to the Milky Way, such as the so-called classical dwarfs [62].

We carry out fits to σ_T/m_χ and σ_V/m_χ. For a given $v_{\rm rel}$, these cross sections depend on two parameters, which are thus determined by the fits to the data. Since the small-$\beta_{\rm rel}$ limit (which is also the $r \to 0$ limit for a given ratio m_χ/m_ξ) of our σ_T in Eq. (2.4) is

$$\lim_{r\to 0} \sigma_T = 2\pi\sigma_0, \tag{3.1}$$

so that

$$\lim_{r\to 0} \frac{\sigma_T}{m_\chi} = \frac{2\pi\alpha_\chi^2 m_\chi}{m_\xi^4}, \tag{3.2}$$

we take one fitting parameter to be

$$\frac{\hat{\sigma}}{m_\chi} \equiv \frac{2\pi\alpha_\chi^2 m_\chi}{m_\xi^4}. \tag{3.3}$$

Here we use the symbol $\hat{\sigma}$ to indicate that this is a fitting parameter. Note also that in the same limit, our σ_V in Eq. (2.5) has the value

$$\lim_{r\to 0} \sigma_V = \frac{2}{3}\lim_{r\to 0} \sigma_T = \frac{4\pi}{3}\sigma_0. \tag{3.4}$$

The other fitting parameter is the ratio

$$\rho_{\chi\xi} \equiv \frac{m_\chi}{m_\xi}, \tag{3.5}$$

which, for a given $v_{\rm rel}$, determines r. For this comparison we utilize the same central values and estimated error bars as in Fig. 1 of [52]. We use a χ^2 fitting procedure in the NonlinearModelFit routine in *Mathematica*, with our formulas (2.4) and (2.5) for the transfer and viscosity cross sections.

Our results are shown as the black curves in Figs. 3(a) and 3(b). From the σ_T fit, we find

$$\frac{\hat{\sigma}}{m_\chi} = 1.1 \pm 0.6 \text{ cm}^2/\text{g}, \qquad \rho_{\chi\phi} = (0.90 \pm 0.41) \times 10^3. \tag{3.6}$$

From the σ_V fit, we find the values

$$\frac{\hat{\sigma}}{m_\chi} = 1.4 \pm 0.7 \text{ cm}^2/\text{g}, \qquad \rho_{\chi\phi} = (0.57 \pm 0.19) \times 10^3. \tag{3.7}$$

The confidence-level contours for these fits are shown in Figs. 2(a) and 2(b). The values of χ^2/d.o.f. are 1.40 and 1.35 for the transfer and viscosity cross-section fit, respectively. Here, the number of degrees of freedom (d.o.f.) is equal to the number of data points minus the number of free parameters $= 18 - 2 = 16$. These χ^2/d.o.f. values indicate

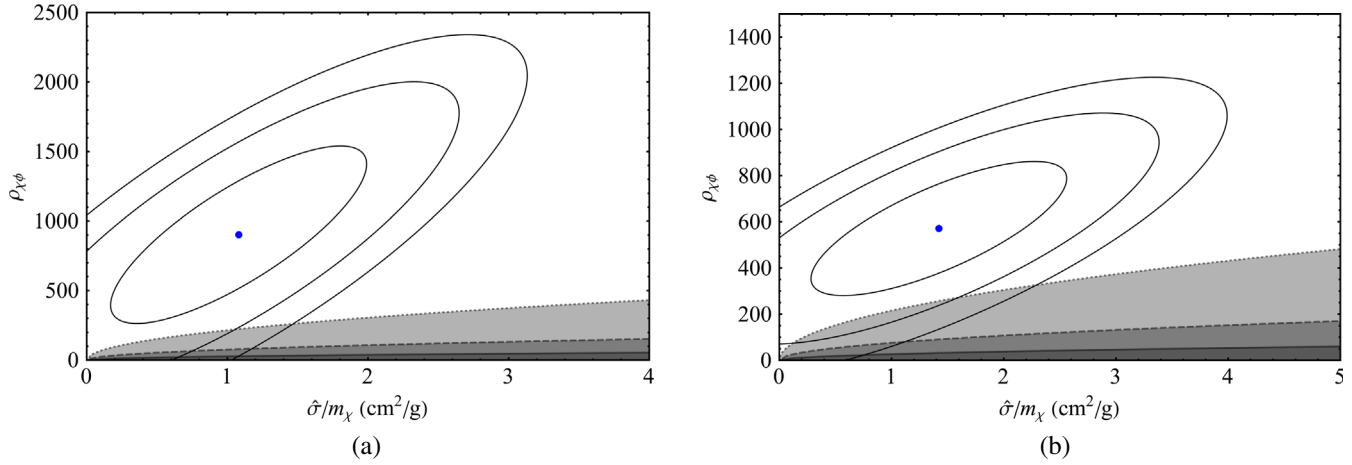

FIG. 2. Plots showing 68%, 95%, and 99% confidence-level (C.L.) contours (the inner, middle, and outer curves, respectively) for the fitting parameters $\rho_{\chi\xi}$ and (a) $\hat{\sigma}_T/m_\chi$ and (b) $\hat{\sigma}_V/m_\chi$. In each figure, the blue point denotes the respective best-fit point. The curves show the boundaries between the parameter regions where our Born calculation is applicable (light regions) and inapplicable (dark regions) for the illustrative mass values $m_\chi = 1, 2, 4$ GeV, with the larger excluded regions applying for larger m_χ. See text and caption to Fig. 1 for further details.

that the fits are reasonably good. As a check on this fitting procedure, we also performed a orthogonal distance regression (ODR) in PYTHON, utilizing the scipy.odr module, where instead of the least square distances, the ODR minimizes the sum of squared perpendicular distances of each data point from the fitted curve. Within the uncertainties in the fitted parameters, we find good agreement between these two fitting methods. We have checked that these fitted values are consistent with our perturbative calculation, i.e., that they are in the Born regime. As discussed in Appendix A of [89], the condition for the validity of the Born approximation is that the quantity $\alpha_\chi m_\chi/m_\xi \equiv \alpha_\chi \rho_{\chi\xi}$ should be small compared with unity. This quantity can be expressed in terms of our fitting parameters $\hat{\sigma}/m_\chi$ and $\rho_{\chi\xi}$, together with m_χ, as

$$\alpha_\chi \rho_{\chi\xi} = \left[\left(\frac{\hat{\sigma}/m_\chi}{2\pi\rho_{\chi\xi}^2}\right) m_\chi^3\right]^{1/2}. \tag{3.8}$$

We have plotted curves along which $\alpha_\chi \rho_{\chi\xi} = 1$ for three illustrative values, $m_\chi = 1, 2, 4$ GeV in Figs. 2 and 4. The dark regions are outside the Born regime. Thus, for values of m_χ of a few GeV, as is plausible in asymmetric DM models, our fitted values are consistent with the Born approximation that we use. A similar comment applies to our other fits given in this paper. For m_χ values outside this range, our Born analysis would not apply. We emphasize that our analysis only applies for model parameters that are in the Born regime and that also lead to sufficient depletion of the symmetric dark matter density. Our results do not exclude m_χ values larger than this range of a few GeV, and the values of $\hat{\sigma}/m_\chi$ and $\rho_{\chi\xi}$ could be different in these cases. For example, Ref. [79] obtained fits to observational data in a light scalar mediator model with $\alpha_\chi = 0.5$, $m_\chi = 190$ GeV, and $m_\phi = 3$ MeV. Since the quantity $\alpha_\chi \rho_{\chi\xi} = 3.2 \times 10^4$ in this case (far outside the Born regime), this shows that it is possible to fit data in a light-mediator SIDM model with quite different values of model parameters.

To address the question posed in this paper, we have carried out corresponding fits to these data using the cross sections $\sigma_{T,\rm lit}$ and $\sigma_{V,\rm lit}$ obtained by including only the t-channel contributions. These are shown as the dashed orange curves in Figs. 1(a) and 1(b), respectively. The small-$\beta_{\rm rel}$ limits (i.e., $r \to 0$ limits, for a fixed ratio m_χ/m_ξ) of $\sigma_{T,\rm lit}$ and $\sigma_{V,\rm lit}$ are given by

$$\lim_{r\to 0} \sigma_{T,\rm lit} = 4\pi\sigma_0 \tag{3.9}$$

and

$$\lim_{r\to 0} \sigma_{V,\rm lit} = \frac{8\pi}{3}\sigma_0, \tag{3.10}$$

which are twice as large as the corresponding small-$\beta_{\rm rel}$ limits of our cross sections. We thus expect that the fitted value of $\hat{\sigma}/m_\chi$ using the results (2.7) and (2.9) will be roughly half the value obtained with the correct formula, and this is borne out by our analysis. With the $\sigma_{T,\rm lit}$ in Eq. (2.7), our fit to these data, shown in Fig. 1(a), yields

$$\frac{\hat{\sigma}}{m_\chi} = 0.45 \pm 0.25 \text{ cm}^2/\text{g}, \quad \rho_{\chi\phi} = (0.42 \pm 0.12) \times 10^3. \tag{3.11}$$

With the $\sigma_{V,\rm lit}$ in Eq. (2.9), our fit to the data, as shown by the dashed orange curve in Fig. 1(b), gives

$$\frac{\hat{\sigma}}{m_\chi} = 0.70 \pm 0.35 \text{ cm}^2/\text{g}, \quad \rho_{\chi\phi} = (0.51 \pm 0.16) \times 10^3. \tag{3.12}$$

For both of these fits, the reduced $\chi^2/\text{d.o.f.} = 1.35$. Again, these $\chi^2/\text{d.o.f.}$ values show that these are reasonably good fits, albeit with the above-mentioned differences in the values of the fitting parameters. Our curves are also consistent with the results of [77], which used modeling methods and simulation taking into account both baryon effects and SIDM.

As we pointed out in [89], for values of $v_{\rm rel} \gtrsim 2 \times 10^3$ km/s typical of galaxy clusters, our σ_T is considerably larger than the result (2.7), and this is evident in the deviation between the black curve and orange dashed curve in Fig. 1(a). However, with the current dataset, this deviation does not have much effect on our fit, since the galaxy clusters have $v_{\rm rel}$ values between $\sim 1 \times 10^3$ km/s and 2×10^3 km/s. It is also possible that σ_T overestimates the effects of SIDM self-scattering when one includes both t-channel and u-channel contributions.

In [89] we calculated that $\sigma_V/\sigma_V^{(t)} = 1 + (1/10)r^2 + O(r^3)$ for $r \ll 1$ and $\sigma_V/\sigma_V^{(t)} = 2 = (1/\ln r)$ for $r \gg 1$ [see Eqs. (4.44) and (4.45) of [89]]. Thus, not only for small r, but also for $r \gtrsim 1$, $\sigma_V^{(t)}$ and σ_V have rather similar functional dependence on r and hence also on $v_{\rm rel}$. This similarity property, shown in [89], is again evident in Fig. 1(b). However, since $\sigma_{V,\rm lit}$ is twice as large as our $\sigma_V^{(t)}$ from [Eq. (4.36) of [89]], a fit of σ_V, lit is expected to yield a value of the fitting parameter $\hat{\sigma}/m_\chi$ that is approximately half as large as a value obtained from a fit using our σ_V, and this expectation is again borne out by our results.

It is also of interest to compare the values of σ_T/m_χ and σ_V/m_χ from our fit to data with the illustrative set of values that we used in [89]. In that paper we utilized the input values $m_\chi = 5$ GeV, $m_\xi = 5$ MeV, and $\alpha_\chi = 3 \times 10^{-4}$. This set of parameters yielded the values 0.99, 0.89, and

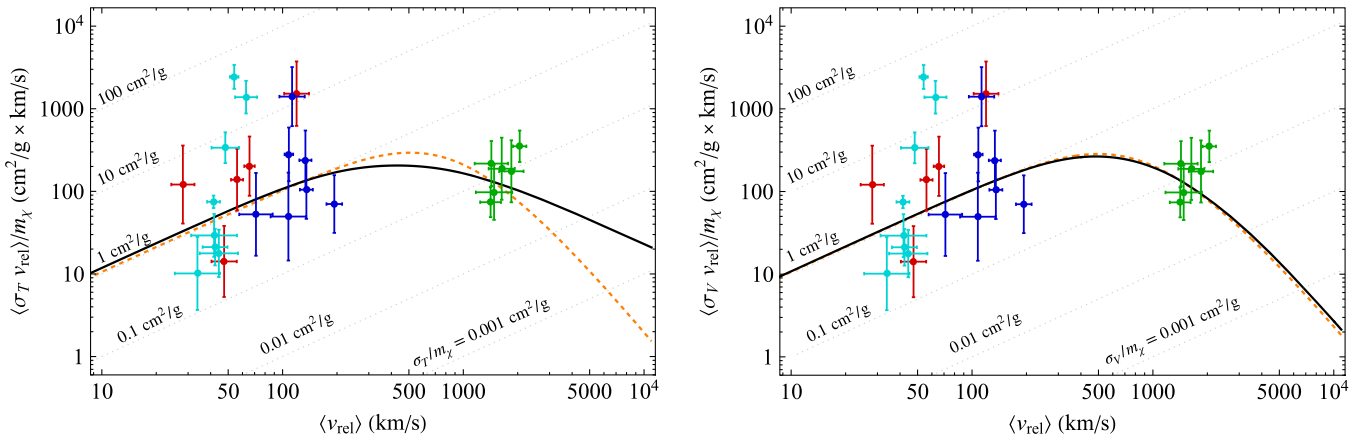

FIG. 3. Fit (black curve) of our (a) σ_T/m_χ and (b) σ_V/m_χ to observational data augmented by inclusion of Milky Way dwarfs, where σ_T and σ_V are given in Eqs. (2.4) and (2.5). The data are from field dwarfs (red), LSB galaxies (blue), galaxy clusters (green), and classical Milky Way dwarfs (cyan), the latter from Ref. [62]. For comparison, fits to the σ_T/m_χ and σ_V/m_χ to this dataset, where σ_T and σ_V are given in Eqs. (2.7) and (2.9) based on Eq. (2.6), are shown as the dashed orange curves. Note that Ref. [88] finds that σ_V provides a better description of thermalization effects due to SIDM scattering than σ_T.

0.13 in units of cm^2/g for σ_T/m_χ and the values 0.66, 0.59, and 0.030 in units of cm^2/g for σ_V/m_χ, for $v_{\rm rel} = 10$, 10^2, and 10^3 km/s, respectively (see Table 1 of [89]). Evidently, these values from [89] are close to results of the actual fit to observational data that we have carried out here. The value of $\rho_{\chi\xi}$ from our fit to σ_T/m_χ is in very good agreement, to within the uncertainty, with the value $\rho_{\chi\xi} = 10^3$ for the illustrative set in [89], while the value of $\rho_{\chi\xi}$ from our fit to σ_V/m_χ is slightly smaller than the above-mentioned illustrative value in [89] but is well within the Born regime shown in Fig. 3 of [89].

It is also worthwhile to consider fits to a larger set of astronomical data. For this purpose, we have carried out the analogous fits of σ_T/m_χ and σ_V/m_χ to a dataset consisting of the above objects (field dwarfs, LSB galaxies, and galaxy clusters) considered in [52] augmented by the classical Milky Way dwarf spheroidal (dSph) galaxies, as analyzed in [62], namely Ursa Minor, Draco, Sculptor, Sextans, Carina, Fornax, Leo I, and Leo II), with distances ranging from 76 kpc (for Draco) to 254 kpc (for Leo I) [95]. Since these classical dSph galaxies are closer to the disk of the Milky Way than the field dwarfs that were fitted in [52], they are more susceptible to environmental effects due to the Milky Way, including tidal stripping, than these more distant field dwarfs, as was cautioned in [62] and has been studied further in [78,84].

With these caveats in mind, we show our results in Figs. 3(a) and 3(b). The corresponding confidence-level contour plots are presented in Figs. 4(a) and 4(b). As is evident, there is considerable scatter in the data in this larger dataset. The best fit parameters that we find for this dataset are

$$\frac{\hat{\sigma}}{m_\chi} = 1.2 \pm 0.7 \text{ cm}^2/\text{g}, \quad \rho_{\chi\phi} = (0.96 \pm 0.54) \times 10^3 \tag{3.13}$$

and

$$\frac{\hat{\sigma}}{m_\chi} = 1.6 \pm 0.9 \text{ cm}^2/\text{g}, \qquad \rho_{\chi\phi} = (0.61 \pm 0.25) \times 10^3. \tag{3.14}$$

The corresponding values of χ^2/d.o.f. for the fit to this larger dataset are 2.92 and 2.76 for the transfer and viscosity cross sections, respectively. The increase in χ^2/d.o.f., i.e., reduction in the goodness of fit, is presumably associated with the greater scatter (diversity) in the Milky Way dSph dataset from [62]. This scatter may be understood better as a result of improved modeling of these Milky Way dwarfs [78,84] (and references therein).

With the $\sigma_{T,\rm lit}$ and $\sigma_{V,\rm lit}$ in Eqs. (2.7) and (2.9) used for the theoretical model, the fit parameters are

$$\frac{\hat{\sigma}}{m_\chi} = 0.5 \pm 0.3 \text{ cm}^2/\text{g}, \quad \rho_{\chi\phi} = (0.44 \pm 0.17) \times 10^3 \tag{3.15}$$

and

$$\frac{\hat{\sigma}}{m_\chi} = 0.8 \pm 0.4 \text{ cm}^2/\text{g}, \quad \rho_{\chi\phi} = (0.54 \pm 0.21) \times 10^3. \tag{3.16}$$

The reduced χ^2/d.o.f. values for these fits are 2.73 and 2.74, respectively. Note that for the larger dataset, d.o.f. $= 26 - 2 = 24$. In future work, one could further

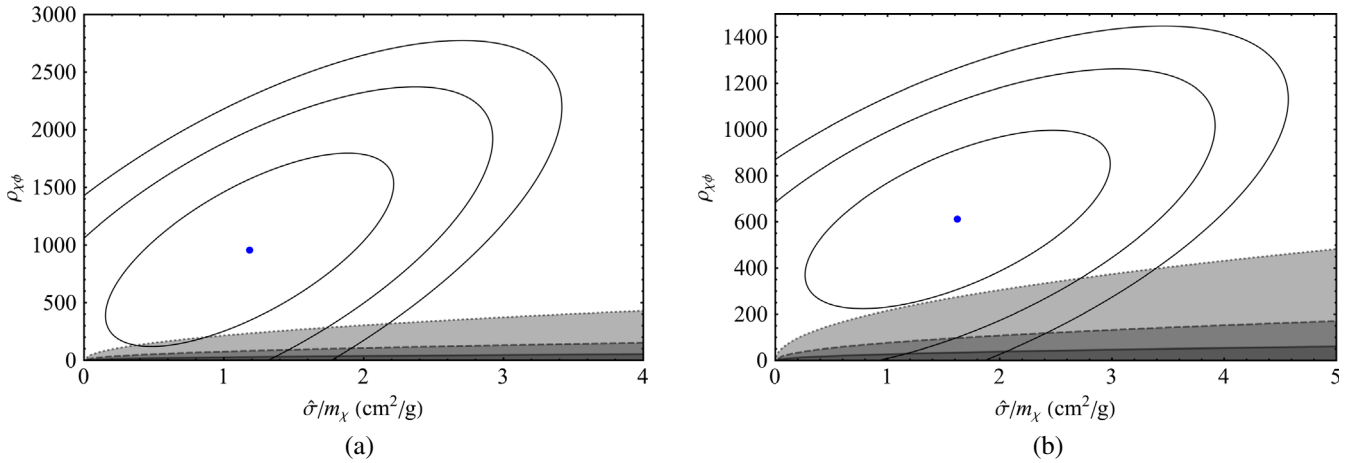

FIG. 4. Plots showing 68%, 95%, and 99% C.L. contours for the fitting parameters $\rho_{\chi\xi}$ and (a) $\hat{\sigma}_T/m_\chi$ and (b) $\hat{\sigma}_V/m_\chi$ for the observational data including Milky Way dwarf galaxies from [62]. In each figure, the blue point denotes the respective best-fit point. The curves show the boundaries between the parameter regions where our Born calculation is applicable (light regions) and inapplicable (dark regions) for the illustrative mass values $m_\chi = 1, 2, 4$ GeV, with the larger excluded regions applying for larger m_χ. See text and caption to Fig. 3 for further details.

enlarge the datasets for SIDM fits. Indeed, several dedicated observational surveys have considerably expanded the number of Milky Way dwarf satellites in recent years, in particular, with the detection of ultrafaint dwarfs [95,96].

It is useful to consider a rescaling of parameters for the cross sections based on inclusion of only the t-channel contribution for $\sigma_{T,\mathrm{lit}}$, Eq. (2.7), and for $\sigma_{V,\mathrm{lit}}$, Eq. (2.9), that minimizes the respective deviations from the cross sections calculated with inclusion of both t-channel and u-channel contributions (and their interference), given by Eqs. (2.4) for σ_T and by Eq. (2.5) for σ_V. For this purpose, we use our fit to the observational data in [52]. We find that an overall rescaling of $\sigma_0 \to (1/2)\sigma_0$ and $r \to 0.75r$ for the fit with $\sigma_{V,\mathrm{lit}}$ in Eq. (2.9) numerically minimizes its deviation from the results obtained with σ_V in Eq. (2.5). Here the factor of $1/2$ accounts for the identical final-state particles. Note that this rescaling is consistent with the best fit obtained in Eqs. (3.7) and (3.12). Furthermore, from Eq. (2.1), if one fixes m_χ, then the above rescaling implies a slight shift in the underlying physical parameters, namely $m_\xi \to 1.15m_\xi$ and $\alpha_\chi \to 0.94\alpha_\chi$. In order to minimize the deviation of cross sections in Eqs. (2.7) and (2.5), we can rescale $\sigma_0 \to \sigma_0/3$ and $r \to 0.45r$. The rescaling $\sigma_0 \to \sigma_0/3$ can be understood as the combination of the factor $2/3$ coming from the different weights in the definition of transfer and viscosity cross section and the factor $1/2$ to account for the identical final-state particles. Similarly, this implies a slight rescaling of $\alpha_\chi \to 1.28\alpha_\chi$ and $m_\xi \to 1.49m_\xi$. This agrees with our best fits in Eqs. (3.7) and (3.11). These rescalings can be useful to estimate the conversion of results in the literature, based on inclusion of only t-channel contributions, to results from calculations of cross sections based on inclusion of both the t-channel and u-channel terms in the Born regime.

IV. CONCLUSIONS

In conclusion, self-interacting dark matter models provide an appealing way to avoid problems encountered in pure cold dark matter simulations lacking baryon feedback. In this paper we have continued our study of an asymmetric dark matter model with self-interactions, in the Born parameter regime. In [89] we calculated differential and integrated cross sections that take into account both t-channel and u-channel contributions to the scattering of identical dark matter fermions via exchange of a light mediator particle. Our work in [89] was motivated in part by the previous use of cross-section formulas that included only t-channel contributions in fits to astronomical data. Here we have investigated a question that arose from our analysis in [89], namely how the results of these fits change when one uses cross sections that correctly include both t-channel and u-channel contributions. Our results for the fitting parameters $\hat{\sigma}/m_\chi$ and $\rho_{\chi\xi}$ are somewhat different from the values that one would get if one were to use only t-channel contributions. Nevertheless, our broad conclusions are in agreement with previous studies, namely that this type of self-interacting dark matter model with a light mediator can provide a reasonably good fit to a variety of observational data ranging from dwarfs to galaxy clusters. Further progress in modeling and comparison of SIDM models with observational data should shed additional light on this promising class of dark matter models.

ACKNOWLEDGMENTS

We thank Dr. Mauro Valli for valuable discussions and Professor Hai-Bo Yu for useful email exchanges. This research was supported in part by the U.S. National Science Foundation Grants No. NSF-PHY-19-15093 and No. NSF-PHY-22-10533 (R. S.) and by support from Tsung-Dao Lee Institute (S. G.).

[1] G. R. Blumenthal, S. M. Faber, J. R. Primack, and M. J. Rees, Nature (London) **311**, 517 (1984).
[2] J. F. Navarro, C. S. Frenk, and S. D. M. White, Astrophys. J. **462**, 563 (1996).
[3] J. F. Navarro, C. S. Frenk, and S. D. M. White, Astrophys. J. **490**, 493 (1997).
[4] A. V. Kravtsov, A. A. Klypin, J. S. Bullock, and J. R. Primack, Astrophys. J. **502**, 48 (1998).
[5] B. Moore, S. Ghigna, F. Governato, G. Lake, T. R. Quinn, J. Stadel, and P. Tozzi, Astrophys. J. Lett. **524**, L19 (1999).
[6] J. Wang, S. Bose, C. S. Frenk, L. Gao, A. Jenkins, V. Springel, and S. D. M. White, Nature (London) **585**, 39 (2020).
[7] G. Jungman, M. Kamionkowski, and K. Griest, Phys. Rep. **267**, 195 (1996).
[8] J. Binney and S. Tremaine, *Galactic Dynamics* (Princeton University Press, Princeton, NJ, 2008).
[9] G. Bertone, D. Hooper, and J. Silk, Phys. Rep. **405**, 279 (2005).
[10] L. E. Strigari, Phys. Rep. **531**, 1 (2013).
[11] M. Lisanti, in *Proceedings of the Theoretical Advanced Study Institute in Elementary Particle Physics (TASI 2015)* (World Scientific, Singapore, 2017), pp. 399–446.
[12] G. Bertone and D. Hooper, Rev. Mod. Phys. **90**, 045002 (2018).
[13] M. R. Buckley and A. H. G. Peter, Phys. Rep. **761**, 1 (2018).
[14] D. N. Spergel and P. J. Steinhardt, Phys. Rev. Lett. **84**, 3760 (2000).
[15] M. Boylan-Kolchin, J. S. Bullock, and M. Kaplinghat, Mon. Not. R. Astron. Soc. **422**, 1203 (2012).
[16] M. Boylan-Kolchin, J. S. Bullock, and M. Kaplinghat, Mon. Not. R. Astron. Soc. **415**, L40 (2011).
[17] K. M. Zurek, Phys. Rep. **537**, 91 (2014).
[18] S. Tulin and H.-B. Yu, Phys. Rep. **730**, 1 (2018).
[19] S. Adhikari *et al.*, arXiv:2207.10638.
[20] V. Springel, Mon. Not. R. Astron. Soc. **364**, 1105 (2005).
[21] V. Springel *et al.*, Nature (London) **435**, 629 (2005).
[22] C. Scannapieco *et al.*, Mon. Not. R. Astron. Soc. **423**, 1726 (2012).
[23] T. K. Chan, D. Kereš, J. Oñorbe, P. F. Hopkins, A. L. Muratov, C. A. Faucher-Giguère, and E. Quataert, Mon. Not. R. Astron. Soc. **454**, 2981 (2015).
[24] A. R. Wetzel, P. F. Hopkins, J.-h. Kim, C.-A. Faucher-Giguere, D. Keres, and E. Quataert, Astrophys. J. Lett. **827**, L23 (2016).
[25] T. Sawala *et al.*, Mon. Not. R. Astron. Soc. **457**, 1931 (2016).
[26] J. S. Bullock and M. Boylan-Kolchin, Annu. Rev. Astron. Astrophys. **55**, 343 (2017).
[27] S. Y. Kim, A. H. G. Peter, and J. R. Hargis, Phys. Rev. Lett. **121**, 211302 (2018).
[28] A. Fitts *et al.*, Mon. Not. R. Astron. Soc. **490**, 962 (2019).
[29] K. E. Chua, A. Pillepich, M. Vogelsberger, and L. Hernquist, Mon. Not. R. Astron. Soc. **484**, 476 (2019).
[30] F. Governato, A. Zolotov, A. Pontzen, C. Christensen, S. H. Oh, A. M. Brooks, T. Quinn, S. Shen, and J. Wadsley, Mon. Not. R. Astron. Soc. **422**, 1231 (2012).
[31] A. Zolotov, A. M. Brooks, B. Willman, F. Governato, A. Pontzen, C. Christensen, A. Dekel, T. Quinn, S. Shen, and J. Wadsley, Astrophys. J. **761**, 71 (2012).
[32] J. Prada, J. E. Forero-Romero, R. J. J. Grand, R. Pakmor, and V. Springel, Mon. Not. R. Astron. Soc. **490**, 4877 (2019).
[33] A. Lazar *et al.*, Mon. Not. R. Astron. Soc. **497**, 2393 (2020).
[34] R. Dave, D. N. Spergel, P. J. Steinhardt, and B. D. Wandelt, Astrophys. J. **547**, 574 (2001).
[35] A. Kusenko and P. J. Steinhardt, Phys. Rev. Lett. **87**, 141301 (2001).
[36] R. N. Mohapatra, S. Nussinov, and V. L. Teplitz, Phys. Rev. D **66**, 063002 (2002).
[37] S. W. Randall, M. Markevitch, D. Clowe, A. H. Gonzalez, and M. Bradac, Astrophys. J. **679**, 1173 (2008).
[38] N. Arkani-Hamed, D. P. Finkbeiner, T. R. Slatyer, and N. Weiner, Phys. Rev. D **79**, 015014 (2009).
[39] J. L. Feng, M. Kaplinghat, and H.-B. Yu, Phys. Rev. Lett. **104**, 151301 (2010).
[40] M. R. Buckley and P. J. Fox, Phys. Rev. D **81**, 083522 (2010).
[41] J. Koda and P. R. Shapiro, Mon. Not. R. Astron. Soc. **415**, 1125 (2011).
[42] M. Vogelsberger, J. Zavala, and A. Loeb, Mon. Not. R. Astron. Soc. **423**, 3740 (2012).
[43] C. Kouvaris, Phys. Rev. Lett. **108**, 191301 (2012).
[44] T. Lin, H.-B. Yu, and K. M. Zurek, Phys. Rev. D **85**, 063503 (2012).
[45] S. Tulin, H.-B. Yu, and K. M. Zurek, Phys. Rev. Lett. **110**, 111301 (2013).
[46] S. Tulin, H.-B. Yu, and K. M. Zurek, Phys. Rev. D **87**, 115007 (2013).
[47] M. B. Wise and Y. Zhang, Phys. Rev. D **90**, 055030 (2014); **91**, 039907(E) (2015).
[48] J. M. Cline, Z. Liu, G. D. Moore, and W. Xue, Phys. Rev. D **90**, 015023 (2014).
[49] K. Petraki, L. Pearce, and A. Kusenko, J. Cosmol. Astropart. Phys. 07 (2014) 039.
[50] F. Kahlhoefer, K. Schmidt-Hoberg, M. T. Frandsen, and S. Sarkar, Mon. Not. R. Astron. Soc. **437**, 2865 (2014).
[51] O. D. Elbert, J. S. Bullock, S. Garrison-Kimmel, M. Rocha, J. Oñorbe, and A. H. G. Peter, Mon. Not. R. Astron. Soc. **453**, 29 (2015).
[52] M. Kaplinghat, S. Tulin, and H.-B. Yu, Phys. Rev. Lett. **116**, 041302 (2016).
[53] K. Blum, R. Sato, and T. R. Slatyer, J. Cosmol. Astropart. Phys. 06 (2016) 021.
[54] P. Ullio and M. Valli, J. Cosmol. Astropart. Phys. 07 (2016) 025.
[55] M. Vogelsberger, J. Zavala, F.-Y. Cyr-Racine, C. Pfrommer, T. Bringmann, and K. Sigurdson, Mon. Not. R. Astron. Soc. **460**, 1399 (2016).
[56] A. Kamada, M. Kaplinghat, A. B. Pace, and H.-B. Yu, Phys. Rev. Lett. **119**, 111102 (2017).
[57] M. Battaglieri *et al.*, arXiv:1707.04591.
[58] F. Kahlhoefer, K. Schmidt-Hoberg, and S. Wild, J. Cosmol. Astropart. Phys. 08 (2017) 003.
[59] R. N. Mohapatra and S. Nussinov, Phys. Lett. B **776**, 22 (2018).
[60] A. Robertson, R. Massey, and V. Eke, Mon. Not. R. Astron. Soc. **467**, 4719 (2017).
[61] A. Robertson *et al.*, Mon. Not. R. Astron. Soc. **476**, L20 (2018).

[62] M. Valli and H.-B. Yu, Nat. Astron. **2**, 907 (2018).
[63] M. A. Buen-Abad, M. Schmaltz, J. Lesgourgues, and T. Brinckmann, J. Cosmol. Astropart. Phys. 01 (2018) 008.
[64] A. Sokolenko, K. Bondarenko, T. Brinckmann, J. Zavala, M. Vogelsberger, T. Bringmann, and A. Boyarsky, J. Cosmol. Astropart. Phys. 12 (2018) 038.
[65] M. Vogelsberger, J. Zavala, K. Schutz, and T. R. Slatyer, Mon. Not. R. Astron. Soc. **484**, 5437 (2019).
[66] A. Robertson, D. Harvey, R. Massey, V. Eke, I. G. McCarthy, M. Jauzac, B. Li, and J. Schaye, Mon. Not. R. Astron. Soc. **488**, 3646 (2019).
[67] T. Ren, A. Kwa, M. Kaplinghat, and H.-B. Yu, Phys. Rev. X **9**, 031020 (2019).
[68] R. Essig, S. D. Mcdermott, H.-B. Yu, and Y.-M. Zhong, Phys. Rev. Lett. **123**, 121102 (2019).
[69] P. Salucci, Astron. Astrophys. Rev. **27**, 2 (2019).
[70] E. O. Nadler, A. Banerjee, S. Adhikari, Y.-Y. Mao, and R. H. Wechsler, Astrophys. J. **896**, 112 (2020).
[71] P. Agrawal, A. Parikh, and M. Reece, J. High Energy Phys. 10 (2020) 191.
[72] K. Hayashi, M. Ibe, S. Kobayashi, Y. Nakayama, and S. Shirai, Phys. Rev. D **103**, 023017 (2021).
[73] K. E. Andrade, J. Fuson, S. Gad-Nasr, D. Kong, Q. Minor, M. G. Roberts, and M. Kaplinghat, Mon. Not. R. Astron. Soc. **510**, 54 (2021).
[74] X. Chu, C. Garcia-Cely, and H. Murayama, J. Cosmol. Astropart. Phys. 06 (2020) 043.
[75] K. Bondarenko, A. Sokolenko, A. Boyarsky, A. Robertson, D. Harvey, and Y. Revaz, J. Cosmol. Astropart. Phys. 01 (2021) 043.
[76] D. Egana-Ugrinovic, R. Essig, D. Gift, and M. LoVerde, J. Cosmol. Astropart. Phys. 05 (2021) 013.
[77] L. Sagunski, S. Gad-Nasr, B. Colquhoun, A. Robertson, and S. Tulin, J. Cosmol. Astropart. Phys. 01 (2021) 024.
[78] O. Slone, F. Jiang, M. Lisanti, and M. Kaplinghat, Phys. Rev. D **107**, 043014 (2023).
[79] B. Colquhoun, S. Heeba, F. Kahlhoefer, L. Sagunski, and S. Tulin, Phys. Rev. D **103**, 035006 (2021).
[80] T. Ebisu, T. Ishiyama, and K. Hayashi, Phys. Rev. D **105**, 023016 (2022).
[81] M. S. Fischer, M. Brüggen, K. Schmidt-Hoberg, K. Dolag, A. Ragagnin, and A. Robertson, Mon. Not. R. Astron. Soc. **510**, 4080 (2022).
[82] T. S. Ray, S. Sarkar, and A. K. Shaw, J. Cosmol. Astropart. Phys. 09 (2022) 011.
[83] A. Zentner, S. Dandavate, O. Slone, and M. Lisanti, J. Cosmol. Astropart. Phys. 07 (2022) 031.
[84] M. Silverman, J. S. Bullock, M. Kaplinghat, V. H. Robles, and M. Valli, Mon. Not. R. Astron. Soc. **518**, 2418 (2022).
[85] D. Eckert, S. Ettori, A. Robertson, R. Massey, E. Pointecouteau, D. Harvey, and I. G. McCarthy, Astron. Astrophys. **666**, A41 (2022).
[86] M. S. Fischer, M. Brüggen, K. Schmidt-Hoberg, K. Dolag, F. Kahlhoefer, A. Ragagnin, and A. Robertson, Mon. Not. R. Astron. Soc. **516**, 1923 (2022).
[87] N. J. Outmezguine, K. K. Boddy, S. Gad-Nasr, M. Kaplinghat, and L. Sagunski, arXiv:2204.06568.
[88] D. Yang and H.-B. Yu, J. Cosmol. Astropart. Phys. 09 (2022) 077.
[89] S. Girmohanta and R. Shrock, Phys. Rev. D **106**, 063013 (2022).
[90] S. Girmohanta and R. Shrock, Phys. Rev. D **104**, 115021 (2021).
[91] S.-H. Oh, W. J. G. de Blok, E. Brinks, F. Walter, and R. C. Kennicutt, Jr., Astron. J. **141**, 193 (2011).
[92] R. Kuzio de Naray, S. S. McGaugh, and W. J. G. de Blok, Astrophys. J. **676**, 920 (2008).
[93] A. B. Newman, T. Treu, R. S. Ellis, D. J. Sand, C. Nipoti, J. Richard, and E. Jullo, Astrophys. J. **765**, 24 (2013).
[94] A. B. Newman, T. Treu, R. S. Ellis, and D. J. Sand, Astrophys. J. **765**, 25 (2013).
[95] A. Drlica-Wagner *et al.* (DES Collaboration), Astrophys. J. **893**, 1 (2020).
[96] J. D. Simon, Annu. Rev. Astron. Astrophys. **57**, 375 (2019).